Title: An N-parallel FENE-P constitutive model and its application in large-eddy simulation of viscoelastic turbulent drag-reducing flow

Authors: Jingfa Li, Bo Yu, Shuyu Sun, Dongliang Sun, Yasuo Kawaguchi

PII: S1877-7503(18)30904-9
DOI: https://doi.org/10.1016/j.jocs.2018.09.016
Reference: JOCS 928

To appear in:

Received date: 16-8-2018
Revised date: 25-9-2018
Accepted date: 29-9-2018

Please cite this article as: Li J, Yu B, Sun S, Sun D, Kawaguchi Y, An N-parallel FENE-P constitutive model and its application in large-eddy simulation of viscoelastic turbulent drag-reducing flow, *Journal of Computational Science* (2017), https://doi.org/10.1016/j.jocs.2018.09.016

An N-parallel FENE-P constitutive model and its application in large-eddy simulation of viscoelastic turbulent drag-reducing flow

Jingfa Li[1, 2], Bo Yu[1], Shuyu Sun[2], Dongliang Sun[1], Yasuo Kawaguchi[3]

[1] School of Mechanical Engineering, Beijing Key Laboratory of Pipeline Critical Technology and Equipment for Deepwater Oil & Gas Development, Beijing Institute of Petrochemical Technology, Beijing 102617, China

[2] Computational Transport Phenomena Laboratory, Division of Physical Science and Engineering, King Abdullah University of Science and Technology, Thuwal 23955-6900, Saudi Arabia

[3] Department of Mechanical Engineering, Tokyo University of Science, Noda-shi, Chiba 278-8510, Japan

(Corresponding authors: +86-10-81292805, yubobox@vip.163.com; +966-2-808 0342, shuyu.sun@kaust.edu.sa)

Highlights

1. An N-parallel FENE-P model based on multiple relaxation times is proposed.
2. Good accuracy and lower computational cost are gained compared to the traditional FENE-P model.
3. Application to large-eddy simulation of the viscoelastic turbulent drag-reducing flow is performed.

Abstract: In this paper, an N-parallel FENE-P constitutive model based on multiple relaxation times is proposed, it can be viewed as a simplified version of the multi-mode FENE-P model under the assumption of identical deformation rate. The proposed model holds the merit of multiple relaxation times to preserve good computational accuracy but could reduce the computational cost, especially in the application of high-fidelity numerical simulation of viscoelastic turbulent drag-reducing flow. Firstly the establishment of N-parallel FENE-P model and the numerical approach to calculate the apparent viscosity are introduced. Then the proposed model is compared with the experimental data and the conventional FENE-P model in estimating rheological properties of two common-used viscoelastic fluids to validate its performance. This work is an extended version of our ICCS conference paper [1]. To further judge the performance of the proposed FENE-P model in complex turbulent flows, the extended application of the proposed model in large-eddy simulation of viscoelastic turbulent drag-reducing channel flow is carried out.

Keywords: N-parallel FENE-P model; Viscoelastic fluid; Multiple relaxation times; Apparent viscosity; Large-eddy simulation.

1. Introduction

In 1948, Toms [2] first reported an interesting phenomenon that adding a little bit of additive, such as some kinds of polymers, into the turbulent flow would induce a drag reduction (DR) in the 1st International Rheology Congress, it was later called turbulent DR effect or Toms' effect. From 1950 to now, as two kinds of successful turbulent drag reducers, the researches on turbulent DR mechanism and industrial applications of the polymer and surfactant have attracted a multitude of scholars' attention all over the world. Among the popular research approaches, numerical simulation has become a powerful tool to get insight into the DR mechanism of the viscoelastic fluid accompanying with rapid developments in mathematical modeling and computer science in recent years. However, distinguishing from the Newtonian fluid, the viscoelastic fluid shows complicated rheological properties and elastic effect. It is a prerequisite to establish a constitutive model that describing the quantitative relation between elastic stress and strain in numerical simulations of viscoelastic turbulent drag-reducing flow. In general, the upper convected Maxwell (UCM) model [3], Oldroyd-B model [4, 5] and Giesekus model [6] as well as the FENE-P model [7] are commonly-used constitutive models in a large number of studies. For the desirable performance to represent the shear-thinning property compared with the UCM and Oldroyd-B models, the Giesekus and FENE-P models have been applied widely. Especially in the FENE-P model the deformation is assumed to be finitely extensible nonlinear, which matches the physical process well.

It is well known that the rheological properties and turbulent DR effect are closely related to the microstructures (such as the long-chain structure in the polymer solution, network structure in surfactant solution, etc.) formed in viscoelastic fluids. Therefore, it is necessary to delve into the validity of the constitutive model from the deformation of microstructures. For the polymer solution, as the Fig. 1(a) shows, the long-chain structure would exert dynamic deformation under the shear effect in flow, sometimes they would tangle with each other [8]. Different from the polymer solution, the DR effect of surfactant solution depends on the micelles which are composed of small surfactant molecules. As illustrated in Fig. 1(b), the spherical micelles, rod-like micelles and network structures would be formed in sequence with the increase of the surfactant concentration under shear effect in flow, accompanying with dynamic deformations of microstructures [9]. From above all, it is evident to see that various deformations of microstructures will take place under the shear effect in viscoelastic fluid. The difficulty to deform can be measured by the relaxation time, it reflects the elastic effect strength of the viscoelastic fluid and is a significant parameter in the constitutive model. For the real viscoelastic fluid, the relaxation time has a wide range of scales (called spectral/multiple relaxation times) due to the anisotropy caused by various deformations and configurational states in the shear flow. In theoretical and experimental studies of the DR

effect, however, the multiple relaxation times are always simplified as single relaxation time because of the extra computational cost and sophisticated analysis when multiple relaxation times are considered. Correspondingly, the commonly-used constitutive models mentioned above are characterized by only a single relaxation time, which is inconsistent with the real physical process apparently. It is the main reason that results in deviations between the theoretical, experimental and numerical studies of DR mechanism of viscoelastic turbulent flow.

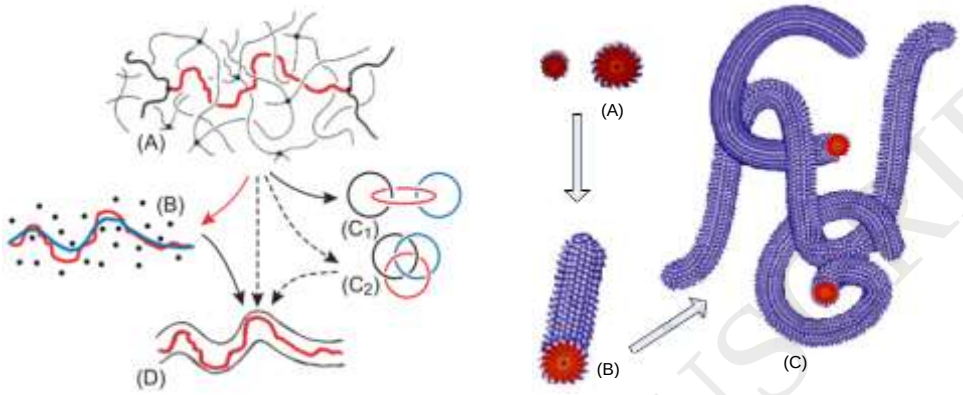

(a) High-molecular polymer solution (b) Surfactant solution

Fig. 1 Schematics of microstructures formed in two viscoelastic fluids

Based on the deformation characteristics of the microstructures in viscoelastic fluid, though the FENE-P model has been illustrated to accurately describe the deformation during unravelled and extended states of the polymer [10–14] and is sufficient for steady flow [15], it is apparent that the traditional FENE-P model with single relaxation time is incapable of accurately characterizing the anisotropy of the deformations or the oscillatory dynamic viscoelasticity. To improve this shortcoming, the multi-mode FENE bead-spring chain model considering multiple relaxation times was proposed and applied to provide a satisfactory description of the polymer dynamics in flows involving a wide range of polymer configurational states [10, 11, 13, 16]. However, these models are rarely used in practice due to their prohibitive computational cost. This limitation would be highlighted especially in the direct numerical simulation (DNS) or large-eddy simulation (LES) of viscoelastic turbulent drag-reducing flow with additives (drag reducer) because extra FENE-P models need to be solved in the simulation.

Therefore, there is a need to develop new or improved multi-mode models which can mimic the dynamics predicted by the FENE chain at a more affordable computational cost. In this study, a simplified multi-mode FENE-P model that we call N-parallel FENE-P model is put forward. The proposed model holds the multiple relaxation times but could relieve the computational burden under the assumption of identical deformation rate in numerical applications. Although this is not the first attempt to empoly the idea of multiple relaxation times (multi-mode) to describe the complex rheological behaviors of viscoelastic fluids, the problem we want to address in

this paper stems from the high-fidelity numerical simulation (such as DNS, LES) of viscoelastic turbulent drag-reducing flow, which has high requirement on the accurate representation of the rheological properties (especially the apparent viscosity) of the viscoelastic fluid. However, it is always contradictory because the additional computational cost would be introduced if the multi-mode FENE-P model is applied. Therefore, it does make sense to improve the multi-mode FENE-P model to gain a good balance between the computational cost and computational accuracy in the simulation. The contribution of this work mainly focuses on two aspects: firstly we propose a simple N-parallel FENE-P model to capture the complex rheological behaviors of viscoelastic fluid with small number mode as least as possible (it needs at least two modes) under the assumption of identical deformation rate for each mode. Fortunately, it is validated with the experimental data and the traditional FENE-P model that our proposed N-parallel FENE-P model is already powerful enough with two contrasted relaxation timescales. Then the double-parallel FENE-P model is applied to the LES of viscoelastic turbulent drag-reducing channel flow. To the best of our knowledge, this is the first attempt that the multi-mode type FENE-P model is employed to the LES study of anisotropic turbulent drag-reducing flow with polymer drag reducer, because for the LES of viscoelastic fluid, the construction of the sub-grid scale (SGS) model is still far from its maturity.

The remainder of this paper is organized as follows. In Section 2, we introduce the establishment of the N-parallel FENE-P constitutive model. The numerical approach to compute the apparent viscosity is briefly presented in Section 3. The validation of the proposed N-parallel FENE-P model with experimental data and traditional FENE-P model is illustrated in Section 4. In Section 5, we apply the double-parallel FENE-P model with two relaxation timescales to the LES of viscoelastic turbulent drag-reducing channel flow. The concluding remarks of this work are summarized in Section 6.

2. Establishment of the N-parallel FENE-P constitutive model

The core idea of the proposed N-parallel FENE-P constitutive model is to put total number N branching FENE-P models in parallel, which enables it holds the multiple relaxation times but could reduce the computational burden in numerical simulations because only one group of deformation rate tensor need to solve. The proposed FENE-P model can describe the rheological behaviors of viscoelastic fluid and characterize the anisotropy of microstructure deformations more accurately. In the following text, the establishment of the improved FENE-P type model is introduced in detail.

To get insight into the rheological properties of the viscoelastic fluid from the microcosmic viewpoint, Bird et al. [7] modeled the polymer macromolecules by using a discrete-element model with the finitely extensible nonlinear elastic (FENE) characteristic, which is also called spring-dumbbell model. The FENE-P constitutive

model is a member of the FENE bead-spring family with Peterlin's approximation [17], and its governing equation reads,

$$\boldsymbol{\tau}_{\mathrm{V}} + \frac{\lambda}{f(r)}\boldsymbol{\tau}_{\mathrm{V}}^{\nabla} = 2\frac{\eta_{\mathrm{V}}}{f(r)}\boldsymbol{D} \tag{1}$$

where $\boldsymbol{\tau}_{\mathrm{V}}$ is the extra elastic stress tensor; λ is the relaxation time; $f(r)$ is a nonlinear factor to ensure the finite extensibility; η_{V} is the zero-shear-rate dynamic viscosity; $\boldsymbol{D}$ is the deformation rate tensor, $\boldsymbol{D} = \left(\nabla\boldsymbol{u} + (\nabla\boldsymbol{u})^{\mathrm{T}}\right)/2$; The triangular superscript '∇' represents the upper-convected derivative symbol.

For more details about the derivation of Eq. (1), readers can refer to [7, 15]. Here we want to point out that the calculation formula of the relaxation time λ reads $\lambda = \xi/4H$, where ξ is the Stokes drag coefficient and H is the Hookean coefficient. If multiple timescales are taken into consideration, the formula can be expressed as $\lambda_i = \xi/4H_i$ (the Stokes drag coefficient is a constant with the same dumbbell in spring-dumbbell model), then the FENE-P model with multiple relaxation time is given by,

$$\boldsymbol{\tau}_{\mathrm{V}i} + \frac{\lambda_i}{f(r_i)}\boldsymbol{\tau}_{\mathrm{V}i}^{\nabla} = 2\frac{\eta_{\mathrm{V}i}}{f(r_i)}\boldsymbol{D}_i \tag{2}$$

where $1 \le i \le N$, N is the total mode number; λ_i , $f(r_i)$ and $\eta_{\mathrm{V}i}$ represent the relaxation time, nonlinear factor and zero-shear-rate dynamic viscosity of the ith branching FENE-P model, respectively.

It can be apparently seen from Eq. (2) that if we apply the M-mode FENE-P model to the simulation, then total (M-1) branching FENE-P models need to be solved additionally, which would result in the heavy computational burden that even cannot afford. In addition, it is clear to observe that the branching FENE-P chains in the multi-mode model are anisotropic, which means the Hookean coefficient H is varied in different branching FENE-P models. This is consistent with the physical process of the deformations. To reduce the computational cost and hold the multiple relaxation times which help to gain better performance at the same time, an N-parallel FENE-P model is proposed in which the deformation rate tensors are simplified as the same. The assumption is reasonable because in the parallel FENE-P model, the Hookean coefficient H measures the difficulty to deform, further the corresponding relaxation times can denote the anisotropy of the deformations in viscoelastic fluid, it is the essential characteristic that depends on the viscoelastic fluid itself, but has nothing to do with the deformation rate $\boldsymbol{D}$. In another word, for different branching FENE-P models with different Hookean coefficients, it takes different relaxation times to achieve the same deformation rate in the parallel model framework. This is the core idea of the proposed FENE-P model in our work.

As illustrated in Fig. 2, when total number N branching FENE-P models are paralleled together, the resulted model satisfies the following characteristics:

(1) The deformation rate tensor $\boldsymbol{D}$ of the N-parallel FENE-P model is identical to that of each branching FENE-P model, this is the main difference from the traditional multi-mode FENE-P model,

$$\boldsymbol{D} = \boldsymbol{D}_1 = \ldots \boldsymbol{D}_i \ldots = \boldsymbol{D}_N \tag{3}$$

(2) The extra elastic stress tensor $\boldsymbol{\tau}_{\mathrm{V}}$ of the N-parallel FENE-P model is equal to the summation of the extra elastic stress tensor $\boldsymbol{\tau}_{\mathrm{V}i}$ of total number N branching FENE-P models,

$$\boldsymbol{\tau}_{\mathrm{V}} = \boldsymbol{\tau}_{\mathrm{V}1} + \ldots + \boldsymbol{\tau}_{\mathrm{V}i} \ldots + \boldsymbol{\tau}_{\mathrm{V}N} = \sum_{i=1}^{N} \boldsymbol{\tau}_{\mathrm{V}i} \tag{4}$$

where the total number of branching FENE-P models $N \geq 2$.

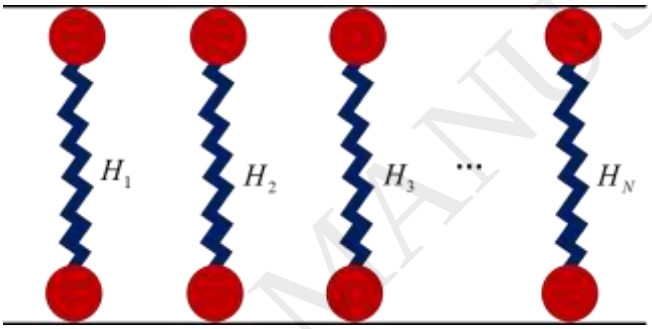

Fig. 2 Schematic of the proposed N-parallel FENE-P model

Substituting Eqs. (2) and (3) into Eq. (4), the governing equation of the N-parallel FENE-P model is then given by,

$$\sum_{i=1}^{N} \boldsymbol{\tau}_{\mathrm{V}i} + \sum_{i=1}^{N} \left(\frac{\lambda_i}{f(r_i)} \boldsymbol{\tau}_{\mathrm{V}i}^{\nabla} \right) = 2 \sum_{i=1}^{N} \frac{\eta_{\mathrm{V}i}}{f(r_i)} \boldsymbol{D} \tag{5}$$

From the above equation, we can find that the N-parallel FENE-P model is a general constitutive model to some extent. For instance, the traditional FENE-P model with single relaxation time can be regarded as an exception of the N-parallel FENE-P model when $N=1$. However, it is different from the multi-mode FENE-P model because when $N \geq 2$ only one group of deformation rate need to solve. It is worth to note that the proposed N-parallel FENE-P model can be rearranged as branching expression form for the convenience of numerical simulation,

$$\begin{cases} \boldsymbol{\tau}_{\mathrm{V}1} + \dfrac{\lambda_1}{f(r_1)}\boldsymbol{\tau}_{\mathrm{V}1}^{\nabla} = 2\dfrac{\eta_{\mathrm{V}1}}{f(r_1)}\boldsymbol{D} \\ \boldsymbol{\tau}_{\mathrm{V}2} + \dfrac{\lambda_2}{f(r_2)}\boldsymbol{\tau}_{\mathrm{V}2}^{\nabla} = 2\dfrac{\eta_{\mathrm{V}2}}{f(r_2)}\boldsymbol{D} \\ \quad\vdots \\ \boldsymbol{\tau}_{\mathrm{V}i} + \dfrac{\lambda_i}{f(r_i)}\boldsymbol{\tau}_{\mathrm{V}i}^{\nabla} = 2\dfrac{\eta_{\mathrm{V}i}}{f(r_i)}\boldsymbol{D} \\ \quad\vdots \\ \boldsymbol{\tau}_{\mathrm{V}N} + \dfrac{\lambda_N}{f(r_N)}\boldsymbol{\tau}_{\mathrm{V}N}^{\nabla} = 2\dfrac{\eta_{\mathrm{V}N}}{f(r_N)}\boldsymbol{D} \end{cases} \tag{6}$$

3. Numerical approach to calculate the apparent viscosity

Apparent viscosity is one of the most significant parameters to measure the rheological properties of viscoelastic fluids. However, a large body of literatures reveal that the conventional constitutive models with single relaxation time show unfavorable performance in describing the apparent viscosity compared with experimental data, especially for unsteady shear flow [15, 18]. To validate whether the proposed N-parallel FENE-P model gains advantage over the traditional one in representing the rheological properties, the numerical approach to compute the apparent viscosity is briefly introduced in this Section.

With certain temperature and solution concentration, the viscosity of viscoelastic fluid is called apparent viscosity or shear viscosity for the reason that it is not a constant but has a close relation to the shear rate. Generally, the expression of the apparent viscosity reads,

$$\eta_a = \tau_{xy} \Big/ \dot{\gamma} = \left(\tau_{\mathrm{N},xy} + \sum_{i=1}^{N} \tau_{\mathrm{V}i,xy} \right) \Big/ \dot{\gamma} \tag{7}$$

where η_a represents the apparent viscosity; $\dot{\gamma}$ denotes the shear rate; $\tau_{\mathrm{N},xy}$, $\sum_{i=1}^{N} \tau_{\mathrm{V}i,xy}$ denote the extra viscous stress contributed by the solvent and solute, respectively.

It can be seen from Eq. (7) that it is a prerequisite to obtain the mathematical relation between $\sum_{i=1}^{N} \tau_{\mathrm{V}i,xy}$ and $\dot{\gamma}$ before calculating the apparent viscosity. In general, water is a commonly-used solvent in viscoelastic fluid and its apparent viscosity can be approximately regarded as constant under specific temperature and solution concentration. Thus the terms $\tau_{\mathrm{N},xy}$ and $\dot{\gamma}$ satisfy the following relation,

$$\tau_{\mathrm{N},xy} = \eta_{\mathrm{N}} \dot{\gamma} \tag{8}$$

where η_{N} denotes the dynamic viscosity of the solvent.

As two successfully drag reducers, the viscosities of the polymer and surfactant change remarkably with the variation of the shear rate. Under certain temperature and solution concentration, the $\sum_{i=1}^{N} \tau_{\mathrm{V}i,xy}$ and $\dot{\gamma}$ satisfy the below relation,

$$\sum_{i=1}^{N} \tau_{\mathrm{V}i,xy} = \sum_{i=1}^{N} \eta_{\mathrm{V}i}(\dot{\gamma})\dot{\gamma} \tag{9}$$

where $\eta_{\mathrm{V}i}(\dot{\gamma})$ represents the dynamic viscosity of the solute.

Substituting Eqs. (8) ~ (9) into Eq. (7), the expression of the apparent viscosity of viscoelastic fluid reads,

$$\eta_a = \eta_{\mathrm{N}} + \sum_{i=1}^{N} \eta_{\mathrm{V}i}(\dot{\gamma}) \tag{10}$$

Therefore, $\sum_{i=1}^{N} \tau_{\mathrm{V}i,xy}$ should be first computed from Eq. (6) to get $\sum_{i=1}^{N} \eta_{\mathrm{V}i}(\dot{\gamma})$. For the sake of concision but without loss of generality, the double-parallel FENE-P model is taken as an example to illustrate the numerical approach to calculate the apparent viscosity. For the convenience, the present study focuses on the two-dimensional simple shear flow (it is applicable to complex shear flow too). Based on the above assumptions, the Eq. (6) and Eq. (10) can be simplified as,

$$\begin{cases} \tau_{\mathrm{V}1,xx} + \tau_{\mathrm{V}2,xx} + \dfrac{\lambda_1}{f(r_1)}\left(\dfrac{\partial \tau_{\mathrm{V}1,xx}}{\partial t} - 2\dfrac{\partial u}{\partial y}\tau_{\mathrm{V}1,xy}\right) + \dfrac{\lambda_2}{f(r_2)}\left(\dfrac{\partial \tau_{\mathrm{V}2,xx}}{\partial t} - 2\dfrac{\partial u}{\partial y}\tau_{\mathrm{V}2,xy}\right) = 0 \\ \tau_{\mathrm{V}1,yy} + \tau_{\mathrm{V}2,yy} + \dfrac{\lambda_1}{f(r_1)}\left(\dfrac{\partial \tau_{\mathrm{V}1,yy}}{\partial t}\right) + \dfrac{\lambda_2}{f(r_2)}\left(\dfrac{\partial \tau_{\mathrm{V}2,yy}}{\partial t}\right) = 0 \\ \tau_{\mathrm{V}1,xy} + \tau_{\mathrm{V}2,xy} + \dfrac{\lambda_1}{f(r_1)}\left(\dfrac{\partial \tau_{\mathrm{V}1,xy}}{\partial t} - \tau_{\mathrm{V}1,yy}\dfrac{\partial u}{\partial y}\right) + \dfrac{\lambda_2}{f(r_2)}\left(\dfrac{\partial \tau_{\mathrm{V}2,xy}}{\partial t} - \tau_{\mathrm{V}2,yy}\dfrac{\partial u}{\partial y}\right) \\ \quad = \dfrac{\eta_{\mathrm{V}1}}{f(r_1)}\left(\dfrac{\partial u}{\partial y}\right) + \dfrac{\eta_{\mathrm{V}2}}{f(r_2)}\left(\dfrac{\partial u}{\partial y}\right) \end{cases} \tag{11}$$

$$\eta_a = \eta_{\mathrm{N}} + \eta_{\mathrm{V}1}(\dot{\gamma}) + \eta_{\mathrm{V}2}(\dot{\gamma}) \tag{12}$$

where the shear rate $\dot{\gamma} = \partial u / \partial y$ for two-dimensional simple shear flow.

The critical step to solve Eq. (11) is discretizing the unsteady term of extra elastic stress. In this paper, the second-order Adams-Bashforth scheme is utilized to discretize the term as below,

$$
\begin{cases}
\tau_{\mathrm{V}i,xx}^{n+1} = \tau_{\mathrm{V}i,xx}^{n} + \dfrac{3}{2}\Delta t\left[2\dot{\gamma}\tau_{\mathrm{V}i,xy}^{n} - \dfrac{f(r_i)^{n}}{\lambda_i}\tau_{\mathrm{V}i,xx}^{n}\right] - \\
\qquad \dfrac{1}{2}\Delta t\left[2\dot{\gamma}\tau_{\mathrm{V}i,xy}^{n-1} - \dfrac{f(r_i)^{n-1}}{\lambda_i}\tau_{\mathrm{V}i,xx}^{n-1}\right] \\
\tau_{\mathrm{V}i,yy}^{n+1} = \tau_{\mathrm{V}i,yy}^{n} - \dfrac{3}{2}\Delta t\left[\dfrac{f(r_i)^{n}}{\lambda_i}\tau_{\mathrm{V}i,yy}^{n}\right] + \dfrac{1}{2}\Delta t\left[\dfrac{f(r_i)^{n-1}}{\lambda_i}\tau_{\mathrm{V}i,yy}^{n-1}\right] \\
\tau_{\mathrm{V}i,xy}^{n+1} = \tau_{\mathrm{V}i,xy}^{n} + \dfrac{3}{2}\Delta t\left[\dot{\gamma}\tau_{\mathrm{V}i,yy}^{n} - \dfrac{f(r_i)^{n}}{\lambda_i}\tau_{\mathrm{V}i,xy}^{n} + \dfrac{\eta_{\mathrm{V}i}}{\lambda_i}\dot{\gamma}\right] - \\
\qquad \dfrac{1}{2}\Delta t\left[\dot{\gamma}\tau_{\mathrm{V}i,yy}^{n-1} - \dfrac{f(r_i)^{n-1}}{\lambda_i}\tau_{\mathrm{V}i,xy}^{n-1} + \dfrac{\eta_{\mathrm{V}i}}{\lambda_i}\dot{\gamma}\right]
\end{cases}
\tag{13}
$$

where the superscript *n* represents the time layer.

The nonlinear factor $f(r_i)$ in Eq. (13) is a function of the conformation tensor. Thus the trace of the conformation tensor should be calculated first,

$$
\mathrm{trace}(c_{\mathrm{V}i}) = c_{\mathrm{V}i,xx}^{n+1} + c_{\mathrm{V}i,yy}^{n+1} \tag{14}
$$

where the conformation tensor components $c_{\mathrm{V}i,xx}^{n+1}$ and $c_{\mathrm{V}i,yy}^{n+1}$ are given as below,

$$
\begin{cases}
c_{\mathrm{V}i,xx}^{n+1} = \left(\dfrac{\lambda_i}{\eta_{\mathrm{V}i}}\tau_{\mathrm{V}i,xx}^{n+1} + 1\right) \Big/ f(r_i)^{n} \\
c_{\mathrm{V}i,yy}^{n+1} = \left(\dfrac{\lambda_i}{\eta_{\mathrm{V}i}}\tau_{\mathrm{V}i,yy}^{n+1} + 1\right) \Big/ f(r_i)^{n}
\end{cases}
\tag{15}
$$

By solving Eqs. (14) and (15), the nonlinear factor of each branching FENE-P model can be computed as,

$$
f(r_i)^{n+1} = \frac{L_i^2 - 3}{L_i^2 - \mathrm{trace}(c_{\mathrm{V}i})} \tag{16}
$$

where L_i^2 denotes the extensibility of the microstructures (such as polymer chain or surfactant network), it is proportional to the ratio of the square of maximum allowable length to the square of the characteristic length of the microstructures in viscoelastic fluids.

Hereafter we can compute the apparent viscosity by solving the N-parallel FENE-P model based on Eqs. (12) ~ (16). The flow chart for the whole computation procedure is shown in Fig. 3.

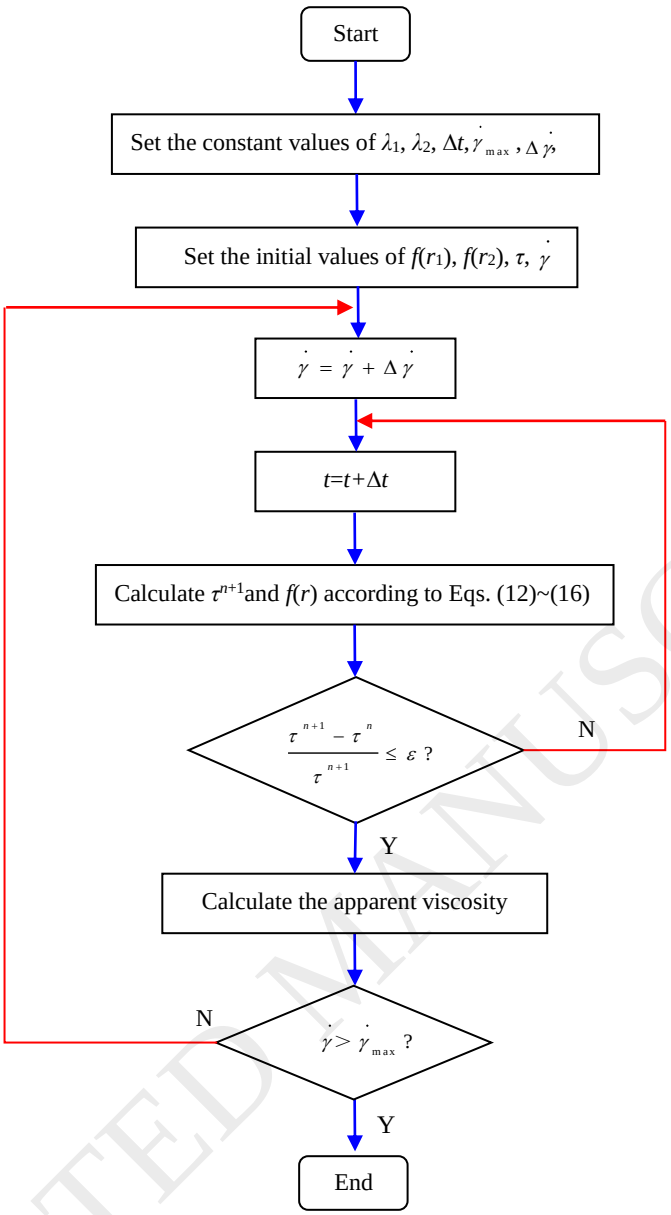

Fig. 3 Flow chart of the numerical calculation of the apparent viscosity

4. Validation of the N-parallel FENE-P constitutive model

4.1 Determination of model parameters

Model parameters of the proposed N-parallel FENE-P model, such as relaxation time λ_i, dynamic viscosity η_{Vi}, should be determined first before the validation. For the sake of the following discussion, we introduce the parameter β_i, which is defined as the ratio of the dynamic viscosity of the *i*th branching FENE-P model (solute) to the zero-shear-rate viscosity of the solvent,

$$\beta_i = \frac{\eta_{Vi}}{\eta_N} \tag{17}$$

The physical meaning of β_i can be regarded as a dimensionless measurement of the solution concentration. The larger the β_i is, the greater the solution concentration is. Hereafter the unknown model parameters of the proposed FENE-P model turn to λ_i and β_i.

For the sake of concision, the double-parallel FENE-P model is taken as an example to illustrate the determination of unknown model parameters. When the experimental data of the apparent viscosity for polymer solution or surfactant solution is obtained, it is easy to get the zero-shear-rate viscosity or apparent viscosity η_α with a certain initial shear rate. For the double-parallel FENE-P model, the apparent viscosity is,

$$\eta_\alpha = \eta_{\mathrm{N}} + \eta_{\mathrm{V1}} + \eta_{\mathrm{V2}} = (1 + \beta_1 + \beta_2)\eta_{\mathrm{N}} \tag{18}$$

The above equation can also be reformulated as,

$$\beta_1 + \beta_2 = \eta_\alpha / \eta_{\mathrm{N}} - 1 \tag{19}$$

The unknown model parameters that need to be determined are β_1 (or β_2) and relaxation times λ_1, λ_2. In general, the experimental data of the apparent viscosity, first normal stress difference, etc., can be measured by rheological experiments. Therefore, the values of apparent viscosity and first normal stress difference can be obtained for the double-parallel FENE-P model. Under this situation, the least square method can be used to determine optimal unknown model parameters. Similarly, the unknown parameters of the N-parallel FENE-P model can be obtained through the least square method too, but it should be noted that more experimental data will be needed with the increase of the total branching number *N*, sometimes it is impractical to obtain these measured data when *N* is too large.

4.2 Results discussion

Figure 4 shows the comparison of the proposed N-parallel FENE-P model (*N*=2) and traditional FENE-P model in describing the apparent viscosity of polymer solutions. In Fig. 4, the independent experimental data sets of polymer solutions with different concentrations are selected from the studies of Ptasinski et al. [19], Hashmet et al. [20] and Pumode et al. [15], respectively. It can be seen that the apparent viscosity of the proposed model agrees better with the experimental data than the traditional model in the shear rate range $0.1s^{-1}$~$1000s^{-1}$, the advantage is remarkable especially when the shear rate is larger than $10s^{-1}$. In addition, the proposed model performs favorable applicability for different concentrations of polymer solutions compared with the conventional model.

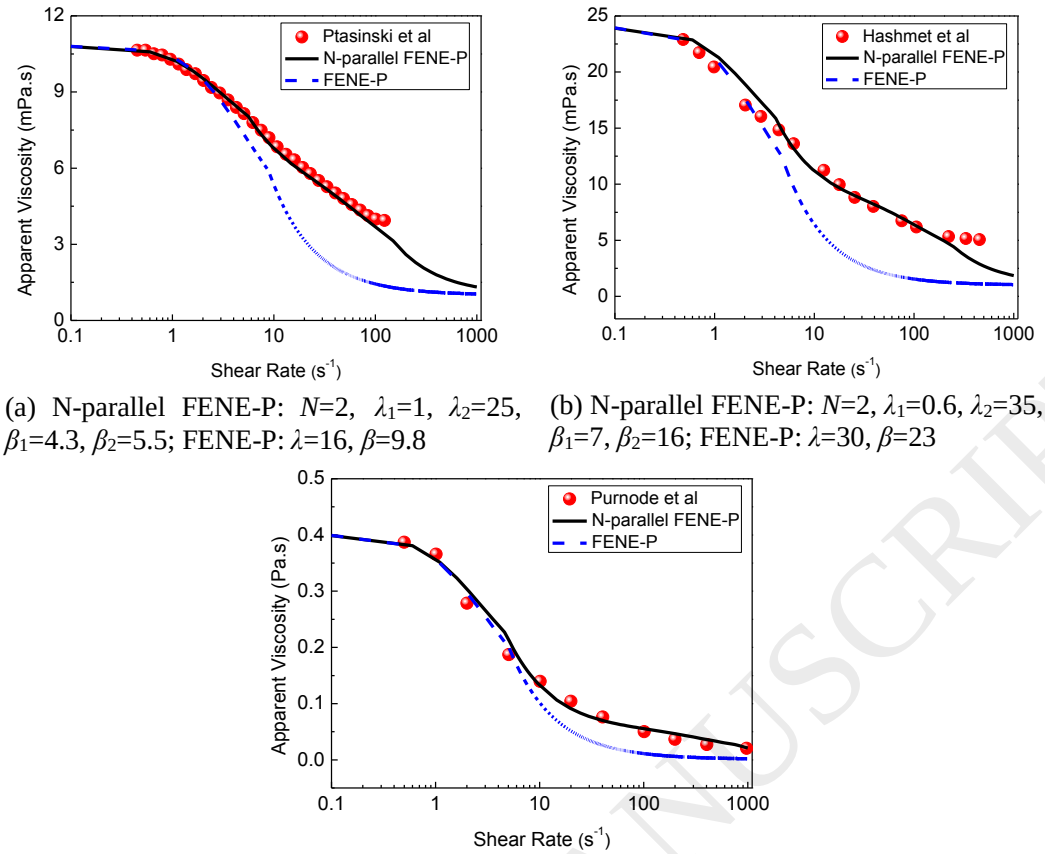

(a) N-parallel FENE-P: N=2, λ_1=1, λ_2=25, β_1=4.3, β_2=5.5; FENE-P: λ=16, β=9.8

(b) N-parallel FENE-P: N=2, λ_1=0.6, λ_2=35, β_1=7, β_2=16; FENE-P: λ=30, β=23

(c) N-parallel FENE-P: N=2, λ_1=0.18, λ_2=30, β_1=49, β_2=350; FENE-P: λ=28, β=399

Fig. 4 Comparison of the N-parallel FENE-P model and traditional FENE-P model in describing the apparent viscosity of polymer solutions

The main reason for the excellent fit can be revealed from the basic idea of the N-parallel FENE-P model. From the microcosmic view, when two branching FENE-P models are paralleled together, the deformation of the microstructures formed in the polymer solution can be controlled and modulated by the representative small relaxation time and large relaxation time simultaneously. The two largely contrasted relaxation times are chosen because the resulting parallel model is capable of representing the broad distribution of timescales in real polymer dynamics. It can reflect the actual deformation characteristics of microstructures more truly and comprehensively. However, for there is only single relaxation time in the traditional FENE-P model, it is limited by the inability to represent multiple timescales corresponding to various deformations and configurational states of the polymer microstructures, which is inconsistent with the physical process. Therefore, the proposed model is more reasonable than the conventional one. Correspondingly, the computational accuracy of the proposed model would be improved considerably.

In addition, we can also find the adjustability of model parameters of the proposed model is much better than that of the traditional model from Fig. 4. The apparent viscosity curves with different shear-thinning rates can be obtained by modulating the model parameters of branching FENE-P models. The increase and decrease of apparent

viscosity curves are influenced more easily by the β_i, the slope of the apparent viscosity curves are affected more obviously by the λ_i.

Figure 5 demonstrates the comparison of proposed model and traditional model in representing the apparent viscosity of surfactant solutions. The experimental data of surfactant solutions with different temperatures and concentrations are chosen from the works of Zhang et al. [21] and Qi et al. [22], respectively. From Fig. 5, it is a pity to see that both the proposed model and the traditional model are incapable of representing the shear thickening behavior of surfactant solutions. The reason for the observed mismatch is that both the proposed N-parallel FENE-P model and the traditional model are all monotonic with regard to the relation between the apparent viscosity and the share rate. The shear thickening property of surfactant solutions can be depicted by the suitable piecewise functional form, such as the viscosity function proposed by Galindo-Rosales et al. [23] which took three characteristic regions (shear thinning, shear thickening and shear thinning) into account separately. However, it requires at least 11 model parameters to determine the piecewise constitutive relation proposed by Galindo-Rosales, which is sometimes impractical in engineering applications. Fortunately, the N-parallel model in our work still offers an obvious advantage over the traditional one in the shear rate range $10s^{-1}$~$1000s^{-1}$. Furthermore, the proposed model can describe the apparent viscosity of surfactant solutions with different temperatures and concentrations, indicating a much wider application.

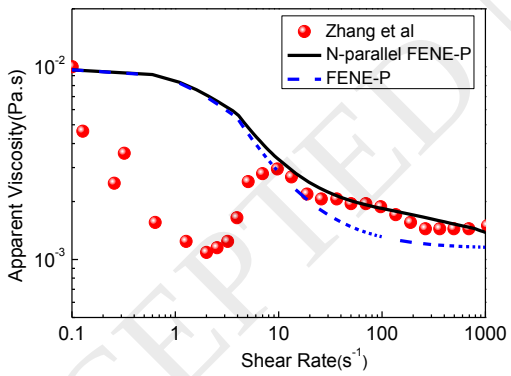

(a) 120ppm, 15℃, η_N=1.1404×10^{-3}Pa.s (N-parallel FENE-P: N=2, λ_1=0.18, λ_2=35.6, β_1=0.5, β_2=7; FENE-P: λ=34.1, β=7.5)

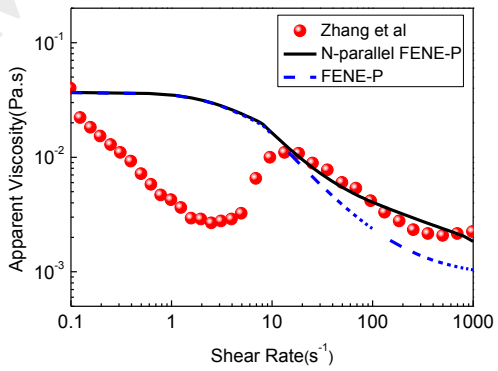

(b) 300ppm, 25℃, η_N=0.8937×10^{-3}Pa.s (N-parallel FENE-P: N=2, λ_1=0.18, λ_2=17.8, β_1=2, β_2=38; FENE-P: λ=17.1, β=40)

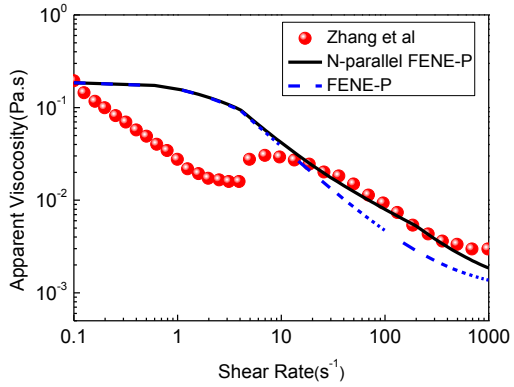

(c) 600ppm, 20℃, η_N=1.0×10^{-3}Pa.s (N-parallel FENE-P: N=2, λ_1=0.71, λ_2=35.6, β_1=5, β_2=180; FENE-P: λ=35.2, β=185)

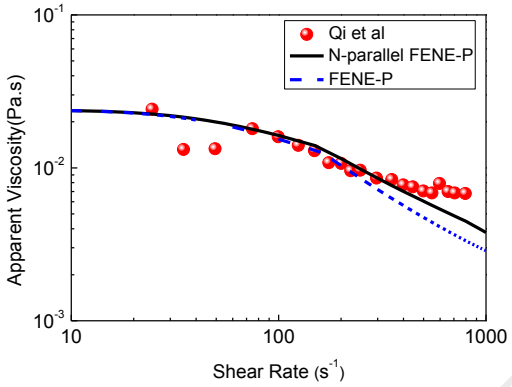

(d) (5 mM/5 mM), 20℃, η_N=1.0×10^{-3}Pa.s (N-parallel FENE-P: N=2, λ_1=0.18, λ_2=0.89, β_1=3, β_2=20; FENE-P: λ=0.87, β=23)

Fig. 5 Comparison of N-parallel FENE-P model and traditional FENE-P model in representing the apparent viscosity of surfactant solutions

The first normal stress difference of the surfactant solution is not equal to zero because the surfactant solution is one of the typical non-Newtonian fluids. Here the comparison of the first normal stress difference is illustrated in Fig. 6. The experimental data are selected from the research of Qi et al. [22], in which the first normal stress difference of surfactant solution Arquad 16-50/NaSal was measured in detail. We can see in Fig. 6 that the estimated first normal stress difference of the proposed model provides an excellent fit to the experimental data, which means the proposed model can represent the first normal stress difference more accurate than the traditional model. Especially when the shear rate is larger than 150s^{-1}, the conventional model can't depict the experimental data accurately, the maximum relative error is approximate 35%.

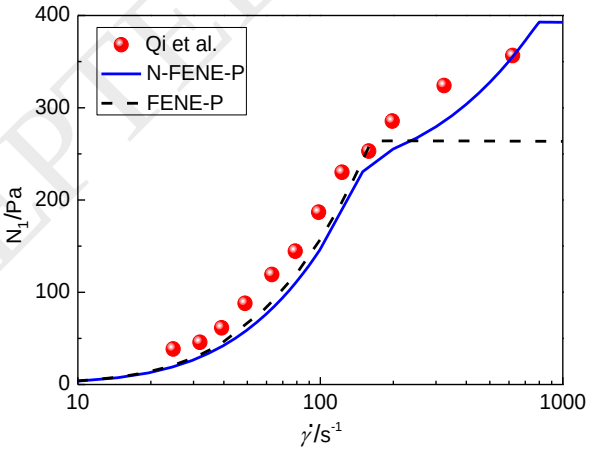

5mM/5mM, 20℃, η_N=1.0×10^{-3}Pa.s (N-parallel FENE-P: N=2, λ_1=0.18, λ_2=0.89, β_1=3, β_2=20; FENE-P: λ=0.87, β=23)

Fig. 6 Comparison of N-parallel FENE-P model and traditional FENE-P model in describing the first normal stress difference of surfactant solution

It is worth pointing out that although the adjustability of the model parameters becomes better and the computational accuracy is improved obviously with the increase

of total branching number N, the computational workload would become heavier following the similar tendency too. Therefore, it is significant to take both the computational accuracy and computational burden into consideration in the determination of the total branching number. N=2 and N=3 are adopted in our numerical experiments and it is found that the computational accuracy of the apparent viscosity with N=3 improved slightly compared with that of N=2. The computational accuracy has already been improved substantially with the representative large relaxation time and small relaxation time than that of the traditional model with single relaxation time, this is the reason why we only present the comparative results with N=2 in this Section.

5. Application in the LES of viscoelastic turbulent drag-reducing flow

To final judge the performance of the proposed N-parallel FENE-P model, in this Section, we apply the proposed model in the real large-eddy simulation of viscoelastic turbulent drag-reducing channel flow, where the shear rate is not uniform in space and time.

5.1 Governing equation

As shown in Fig. 7, the fully developed viscoelastic turbulent drag-reducing channel flow is considered in this work. The sizes of the channel corresponding to the streamwise (x), wall-normal (y) and spanwise (z) directions are 10h, 2h and 5h respectively, where h denotes half-height of the channel.

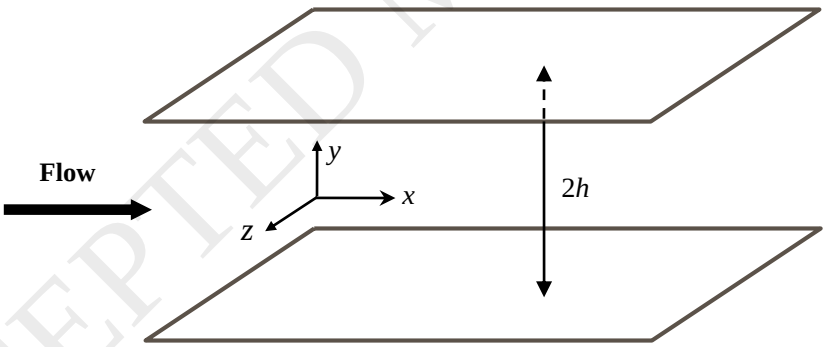

Fig. 7 Schematic of the turbulent drag-reducing channel flow

The governing equation of the viscoelastic turbulent drag-reducing channel flow based on our proposed N-parallel FENE-P model can be written as follows,

$$\frac{\partial u_i}{\partial x_i} = 0 \tag{20}$$

$$\frac{\partial u_i}{\partial t} + u_j \frac{\partial u_i}{\partial x_j} = -\frac{1}{\rho}\frac{\partial p}{\partial x_i} + \frac{\eta_N}{\rho}\frac{\partial}{\partial x_j}\left(\frac{\partial u_i}{\partial x_j}\right) + \sum_{m=1}^{N}\frac{\eta_{Vm}}{\rho\lambda_m}\frac{\partial\left[f(r_m)c_{ij,m}\right]}{\partial x_j} \tag{21}$$

$$\sum_{m=1}^{N}\tau_{\mathrm{V}m,ij}+\sum_{m=1}^{N}\left(\frac{\lambda_m}{f(r_m)}\tau^{\nabla}_{\mathrm{V}m,ij}\right)=2\sum_{m=1}^{N}\frac{\eta_{\mathrm{V}m}}{f(r_m)}D_{ij} \tag{22}$$

where the subscript '*m*' represents the *m*th branching FENE-P model; u_i represents the velocity component; p denotes the pressure; $c_{ij,m}$ denotes the component of conformation tensor; $\eta_{\mathrm{V}m}$, η_{N}, $\tau_{\mathrm{V}m,ij}$, D_{ij}, λ_m and $f(r_m)$ denote the same physical meaning as the variables mentioned in Sections 2~4, $\tau_{\mathrm{V}m}=\frac{n_{\mathrm{V}m}}{\lambda_m}\left(f(r_m)\mathbf{c}-\mathbf{I}\right)$.

For the LES of viscoelastic turbulent flow, the effective sub-grid scale (SGS) model is still far from its maturity up to now. Simulation results have shown the spatial filtering and spatial SGS model that applicable to Newtonian fluid are not suitable to constitutive equation for viscoelastic fluid because of the unsatisfied computational accuracy. Therefore, in this paper, we employ the idea of temporal filtering and temporal SGS model developed by Thais et al. [24] to filter the constitutive equation within time-domain, which is illustrated to yield good numerical accuracy. Compared to the spatial filtering, the temporal filtering has been shown to offer many other advantages except for the accuracy. For example, in LES of turbulence flow, to distinguish the errors that resulted from numerical simulation and numerical mathematical model, the spatial filter width is commonly expected to be larger than the grid size to some extent, however, the spatial filter width is always set as same order of magnitude as grid size in practical numerical researches because the computational cost would increase largely due to the decrease of grid size. For the temporal filtering and temporal SGS model, however, the order of magnitude of filter width can be larger than that of the time step in LES of viscoelastic turbulent flow in the prerequisite of the numerical results are physically meaningful and the computation is stable.

In our large-eddy simulation, the improved mixed sub-grid scale model MICT [25] is applied to filter the Eqs. (20)~(22), in which the improved coherent-structure Smagorinsky model is applied to perform the spatial filtering for the continuity and momentum equations within physical space, and the temporal approximate deconvolution model is applied to perform the temporal filtering for the constitutive equation within time-domain. Here, the half-height *h* of the channel (see Fig. 7) is chosen as the characteristic length and the friction velocity u_τ ($u_\tau=\sqrt{\tau_w/\rho}$) is selected as the characteristic velocity for the nondimensionalization, respectively. The dimensionless form of the filtered LES governing equations reads,

$$\frac{\partial \overline{u}_i^{+}}{\partial x_i^{*}}=0 \tag{23}$$

$$\frac{\partial \overline{u}_i^+}{\partial t^*} + \overline{u}_j^+ \frac{\partial \overline{u}_i^+}{\partial x_j^*} = \delta_{1i} - \frac{\partial \overline{p}^{+'}}{\partial x_i^*} + \frac{1}{Re_\tau} \frac{\partial}{\partial x_j^*} \left(\frac{\partial \overline{u}_i^+}{\partial x_j^*} \right) + \sum_{m=1}^{N} \frac{\beta_m}{We_{\tau,m}} \frac{\partial \left[f(\overline{r}_m) \overline{c}_{ij,m}^+ \right]}{\partial x_j^*} + \sum_{m=1}^{N} \frac{\beta_m}{We_{\tau,m}} \frac{\partial R_{ij,m}}{\partial x_j^*} + \frac{\partial \tau_{ij}}{\partial x_j^*} \tag{24}$$

$$\frac{\partial \overline{c}_{ij,m}^+}{\partial t^*} + \overline{u}_k^+ \frac{\partial \overline{c}_{ij,m}^+}{\partial x_k^*} - \frac{\partial \overline{u}_i^+}{\partial x_k^*} \overline{c}_{kj,m}^+ - \frac{\partial \overline{u}_j^+}{\partial x_k^*} \overline{c}_{ik,m}^+ = \frac{Re_\tau}{We_{\tau,m}} \left[\delta_{ij,m} - f(\overline{r}_m) \overline{c}_{ij,m}^+ \right] + P_{ij,m} + Q_{ij,m} - \frac{Re_\tau}{We_{\tau,m}} R_{ij,m} + \chi_c \left(\overline{\gamma}_{ij,m} - \overline{c}_{ij,m}^+ \right) \tag{25}$$

where the superscript '+' denotes the dimensionless variables; the overbar '-' denotes the filtered variables; Re_τ denotes the friction Reynolds number, $Re_\tau = \rho u_\tau h / \eta_N$; $We_{\tau,m}$ denotes the branching Weissenberg number, $We_{\tau,m} = \lambda_m \rho u_\tau^2 / \eta_N$; τ_{ij} denotes the sub-grid scale shear stress; $R_{ij,m}$ represents a subfilter term related to the nonlinear restoring force; $P_{ij,m}$ and $Q_{ij,m}$ represent subfilter terms induced by stretching of microstructures; $\chi_c \left(\overline{\gamma}_{ij,m} - \overline{c}_{ij,m}^+ \right)$ is a second-order regularization term representing the kinetic energy transfer between the scales that cannot be recovered by deconvolution procedure; χ_c denotes the dissipative coefficient and χ_c =1.0 in this study.

In this paper, the computation of $P_{ij,m}$, $Q_{ij,m}$, $R_{ij,m}$ and $\chi_c \left(\overline{\gamma}_{ij,m} - \overline{c}_{ij,m}^+ \right)$ is not introduced here for brevity, readers can refer to [25] for more details. In the large-eddy simulation, the projection algorithm [25] coupled with the geometric multigrid (GMG) method [26] is adopted to solve the Eqs. (23) ~ (25).

5.2 Cases detail

To evaluate the application performance of the proposed N-parallel FENE-P model, the LES of viscoelastic turbulent drag-reducing channel flow is carried out in present work. Five cases are designed in which case N1 is the Newtonian turbulent channel flow used for comparison and cases V1 ~ V4 have different branching FENE-P model parameters. The detailed dimensionless calculation parameters are presented in Table 1.

In the simulation, the periodic boundary is imposed on streamwise and spanwise directions respectively, the non-slip boundary is set on the wall-normal direction. The initial conditions in the MICT sub-grid scale model and the grid system are set as the same as [25]. In the proposed N-parallel FENE-P model, the L_i^2 representing the extensibility of the polymer chain or surfactant micelles, L_i is set as 100 in this study. The spatial filter width is set as 0.0634 and the temporal filter width is set as $10\Delta t^*$.

Table 1 Calculation parameters

Cases	Δt^*	Re_τ	$We_{\tau,1}$	β_1	$We_{\tau,2}$	β_2
N1	0.0005	600	-	-	-	-
V1	0.0001	600	20	0.1	20	0.1
V2	0.0001	600	40	0.1	40	0.1
V3	0.0001	600	20	0.1	10	0.1
V4	0.0001	600	20	0.1	30	0.1

5.3 Results analysis

In the following content, LES results of the viscoelastic turbulent drag-reducing channel flow using the proposed FENE-P model are presented. It is worth noting that for different calculation conditions are involved in our simulation, limited to the length of the paper but without loss of generality, only some quantities of interest are discussed.

(1) Drag-reduction rate

The drag reduction (DR) effect can largely save energy in the turbulent flow. The DR rate of the viscoelastic turbulent flow can be calculated quantitatively by,

$$\mathrm{DR} = \frac{C_f^D - C_f}{C_f^D} \times 100\% \tag{26}$$

where C_f denotes the Fanning fraction coefficient, $C_f = 2\Big/\left(U_b^+\right)^2$, U_b^+ is the dimensionless mean velocity; C_f^D represents the Fanning fraction coefficient computed using Dean equation, $C_f^D = 0.073 Re_b^{-0.25}$, Re_b is the Reynolds number, $Re_b = 2 Re_\tau U_b^+$.

Table 2 presents the DR results of cases V1 ~ V4 in detail. It can be obviously seen that the DR effect is remarkable under given calculation parameters using the N-parallel FENE-P model, the DR rate all exceed 50% in the four cases. The results indicate the proposed constitutive model is effective in the turbulent drag-reducing flow simulation.

Table 2 Turbulent drag reduction in this study

Cases	Re_b	$C_f/10^{-3}$	$C_f^D/10^{-3}$	DR/%
V1	33287	2.599	5.404	51.91
V2	34369	2.438	5.361	54.52
V3	33492	2.567	5.396	52.42
V4	33389	2.583	5.400	52.15

To further demonstrate the performance of the proposed N-parallel FENE-P model, the DR rate in Table 2 is compared with the literature data. In Table 3, the turbulent DR results in the work of Wang [27] using the traditional FENE-P model are presented. It can be found that under almost same calculation conditions, the DR rate calculated using the

proposed model is 16%~21% higher than that using the traditional model. This is because in the proposed model, the rheological properties can be captured more accurately with the help of multiple relaxation times, which is capable of representing the broad distribution of timescales in the real turbulent flow process.

Table 3 Turbulent drag reduction in literature [27]

Cases	Re_τ	We_τ	β	DR/%
V1	590	10	0.11	32.97
V2	590	20	0.11	35.43

(2) Analysis of frictional resistance coefficient

The contribution of shear stresses on the turbulent frictional resistance of viscoelastic fluid can be computed as follows,

$$C_f = \frac{12}{Re_b} + \frac{6}{\left(U_b^+\right)^2}\int_0^1 \left(-\overline{u}^{+\prime}\overline{v}^{+\prime}\right)\left(1-y^*\right)dy^* + \frac{6}{\left(U_b^+\right)^2}\int_0^1 \sum_{m=1}^{N} \frac{\beta_m f\left(\overline{r}_m\right)\overline{c}_{xy,m}^{+}}{We_{\tau,m}}\left(1-y^*\right)dy^* \quad (27)$$

where on the right-hand side of the equation, the terms from left to right denote the viscous contribution (VC), turbulent contribution (TC) and elastic contribution (EC, represented by N-parallel FENE-P model), respectively. In Newtonian fluids, the EC would be zero.

The statistical histogram for contributions (VC, EC and TC) of different shear stresses on the overall frictional resistance coefficient are illustrated in Fig. 8. We can see that the frictional resistance coefficient of the Newtonian fluid is much larger than that of viscoelastic fluid under the same calculation parameter setting. There is because although the drag reducer would introduce the EC, the TC would be reduced much largely, thus the increase of the EC is smaller than the decrease of the TC. This indicates that the drag reducer added in the turbulent channel flow can largely suppress the turbulence intensity. It can also be seen that the VC of viscoelastic fluid is higher than that of the Newtonian fluid and TC is dominant in both fluids.

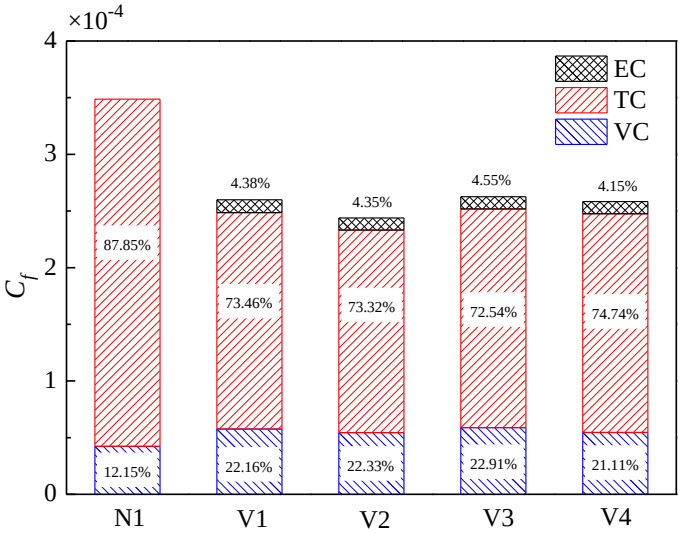

Fig. 8 Statistical histogram of shear stress contributions on the frictional resistance coefficient

(3) Quadrant analysis

Turbulent burst events exert significant influence on the evolution of the turbulent flow. Due to the close relation between Reynolds shear stress and turbulent burst events, a quadrant analysis is carried out for the Reynolds shear stress.

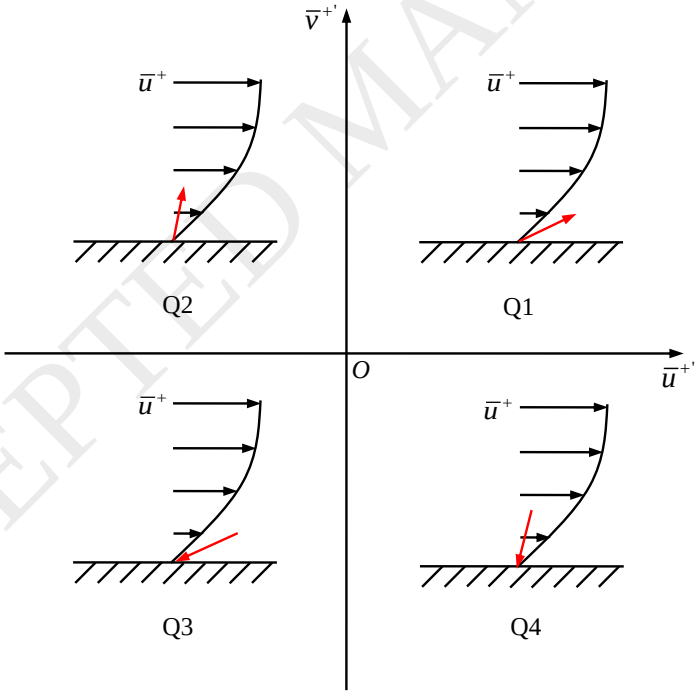

Fig. 9 Schematic diagram of the different turbulent drag-reducing flow motions

Figure 9 displays four types of turbulent flow motions on four quadrants in the $\overline{u}^{+'}-\overline{v}^{+'}$ coordinate system. The 1st quadrant (Q1, $\overline{u}^{+'}>0$, $\overline{v}^{+'}>0$) denotes the high-speed motion and migration of high-momentum fluids away from the near-wall region. The 3rd quadrant (Q3, $\overline{u}^{+'}<0$, $\overline{v}^{+'}<0$) denotes the low-speed motion and

migration of low-momentum fluids toward the near-wall region. The 2nd quadrant (Q2 , $\overline{u}^{+'}<0$, $\overline{v}^{+'}>0$) and the 4th quadrant (Q4 , $\overline{u}^{+'}>0$, $\overline{v}^{+'}<0$) respectively represent the sweep of high-speed fluids and ejection of low-speed fluids caused by the turbulent burst events.

Here the quadrant profiles of the Reynolds shear stress in cases V1 and V2 are depicted in Fig. 10. It can be easily seen the absolute value of Reynolds shear stress of Newtonian fluid is larger than that of viscoelastic fluid in any quadrant, the difference between the two values decreases with the approaching to the channel wall. It is also indicated in Fig. 10 that the sweep of high-speed fluids and ejection of low-speed fluids caused by turbulent burst events are largely suppressed and weakened in the viscoelastic fluid, indicating the decrease of Reynolds shear stress. The high-speed backward motion in 1st quadrant and the low-speed forward motion in the 3rd quadrant are both suppressed and weakened at the same time, whose contributions to the reduction of Reynolds shear stress, however, are much smaller than that of the sweep of high-speed fluids and ejection of low-speed fluids.

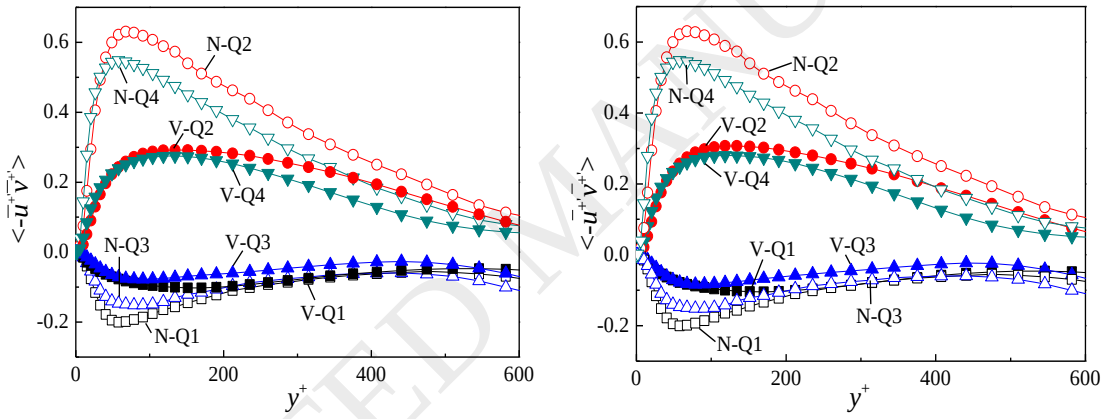

(a) Case V1 (b) Case V2

Fig. 10 Quadrant profiles of Reynolds shear stress
(N represents Newtonian fluid, V represents viscoelastic fluid)

6 Concluding remarks

The present study focuses on the constitutive model describing the rheological properties of viscoelastic fluids and an N-parallel FENE-P model which can be viewed as a simplified multi-mode FENE model is proposed based on multiple relaxation times. The aim of the proposed FENE-P model is to reduce the computational cost of the traditional multi-mode model but preserve good computational accuracy that benefiting from the characteristic of multiple relaxation timescales. The main conclusions of our study can be summarized as fellows:

(1) Compared with the traditional FENE-P model with single relaxation time, the proposed model demonstrates favorable adjustability of the model parameters and wider

application. It utilizes total number *N* branching FENE-P models to describe rheological properties of the viscoelastic fluid and characterize the anisotropy of deformations corresponding to various configurational states, which is more consistent with the real physical process.

(2) The proposed model is shown to perform an excellent fit to independent experimental data sets. It can represent the apparent viscosity of the polymer solution more accurate than the traditional model, the advantage is remarkable especially when the shear rate is in large range. Although the proposed model is also unable to capture the shear thickening of the surfactant solution as the conventional model, it still offers advantages in the large shear rate range.

(3) The proposed model shows good performance in the LES of viscoelastic turbulent drag-reducing flows with drag reducers, which has been validated by the simulation results, such as DR rate, contributions of shear stresses on turbulent frictional resistance, quadrant analysis of the Reynolds shear stress.

Acknowledgments

The study is supported by the National Natural Science Foundation of China (No. 51636006), project of Construction of Innovative Teams and Teacher Career Development for Universities and Colleges under Beijing Municipality (No. IDHT20170507), National Key R&D Program of China (Grant No. 2016YFE0204200), the Program of Great Wall Scholar (CIT&TCD20180313), and the Research Funding from King Abdullah University of Science and Technology (KAUST) through the grants BAS/1/1351-01.

References

1. J. F. Li, B. Yu, S. Y. Sun, D. L. Sun, Study on an N-parallel FENE-P constitutive model based on multiple relaxation times for viscoelastic fluid. In: Y. Shi, H. H. Fu, V. V. Krzhizhanovskaya, M. H. Lees, J. J. Dongarra, P. M. A. Sloot (eds.) ICCS-2018. LNCS 10862 (2018) 610–623, Springer, Heidelberg.
2. B. A. Toms, Some observations on the flow of linear polymer solutions through straight tubes at large Reynolds numbers, Proc. of In. Cong. On Rheology 2 (1948) 135–142.
3. M. Renardy, Y. Renardy, Linear stability of plane Couette flow of an upper convected Maxwell fluid, J. Non-Newtonian Fluid Mech. 22 (1986) 23–33.
4. J. G. Oldroyd, On the formulation of rheological equations of state, Proc. R. Soc. Lond. A 200 (1950) 523–541.
5. P. G. Oliveria, Alternative derivation of differential constitutive equations of the Oldroyd-B type, J. Non-Newtonian Fluid Mech. 160 (2009) 40–46.
6. H. Giesekus, A simple constitutive equation for polymer fluids based on the concept of deformation-dependent tensorial mobility, J. Non-Newtonian Fluid Mech. 11

(1982) 69–109.

7. R. B. Bird, P. J. Dotson, N. L. Johnson, Polymer solution rheology based on a finitely extensible bead-spring chain model, J. Non-Newtonian Fluid Mech. 7, (2-3) (1980) 213–235.
8. R. Everaers, S. K. Sukumaran, G. S. Grest, C. Svaneborg, A. Sivasubramanian, K. Kremer, Rheology and microscopic topology of entangled polymeric liquids, Science 303 (5659) (2004) 823–826.
9. S. Ezrahi, E. Tuval, A. Aserin, Properties, main applications and perspectives of worm micelles, Adv. Colloid Interface Sci. 128-130 (2006) 77–102.
10. P. S. Doyle, E. S .G. Shaqfeh, Dynamic simulation of freely-draining, flexible bead-rod chains: Start-up of extensional and shear flow, J. Non-Newtonian Fluid Mech. 76 (1998) 43–78.
11. P. S. Doyle, E.S.G. Shaqfeh, G.H. McKinley, S.H. Spiegelberg, Relaxation of dilute polymer solutions following extensional flow, J. Non-Newtonian Fluid Mech. 76 (1998) 79–110.
12. M. R. J. Verhoef, B. H. A. A. van den Brule, M. A. Hulsen, On the modelling of a PIB/PB Boger fluid in extensional flow, J. Non-Newtonian Fluid Mech. 80 (1999) 155–182.
13. I. Ghosh, G. H. McKinley, R.A. Brown, R.C. Armstrong, Deficiencies of FENE dumbbell models in describing the rapid stretching of dilute polymer solutions, J. Rheol. 45 (3) (2001) 721–758.
14. Q. Zhou, R. Akhavan, A comparison of FENE and FENE-P dumbbell and chain models in turbulent flow, J. Non-Newtonian Fluid Mech. 109 (2003) 115–155.
15. B. Purnode, M. J. Crochet, Polymer solution characterization with the FENE-P model, J. Non-Newtonian Fluid Mech. 77 (1998) 1–20.
16. L. Li, R.G. Larson, T. Sridhar, Brownian dynamics simulations of dilute polystyrene solutions, J. Rheol. 44 (2) (2000) 291–322.
17. A. Peterlin, Streaming birefringence of soft linear macromolecules with finite chain length, Polymer 2 (1961) 257–264.
18. J. J. Wei, Z. Q. Yao, Rheological characteristic of drag reducing surfactant solution, J. Chemical Industry Eng. (Chinese) 58(2) (2007) 0335–0340.
19. P. K. Ptasinski, F. T. M. Nieuwstadt, B. H. A. A. van den Brule, M. A. Hulsen, Experiments in turbulent pipe flow with polymer additives at maximum drag reduction, Flow, Turbul. Combust. 66 (2001) 159–182.
20. M. R. Hashmet, M. Onur, I. M. Tan, Empirical correlations for viscosity of polyacrylamide solutions with the effects of concentration, molecular weight and degree of hydrolysis of polymer, J. Appl. Sci 14 (10) (2014) 1000–1007.
21. H. X. Zhang, D. Z. Wang, W. G. Gu, H. P. Chen, Effects of temperature and concentration on rheological characteristics of surfactant additive solutions, J. Hydrodyn. 20 (5) (2008) 603–610.

22. Y. Y. Qi, K. Littrell, P. Thiyagarajan, Y. Talmon, J. Schmidt, Z. Q. Lin, Small-angle neutron scattering study of shearing effects on drag-reducing surfactant solutions, J. Colloid Interface Sci. 337 (2009) 218–226.
23. F. J. Galindo-Rosalesa, F. J. Rubio-Hernández, A. Sevilla, An apparent viscosity function for shear thickening fluids, J. Non-Newtonian Fluid Mech. 166 (2011) 321–325.
24. L. Thais, A. E. Tejada-Martínez, T. B. Gatski, G. Mompean, Temporal large eddy simulations of turbulent viscoelastic drag reduction flows, Phys. Fluids 22 (1) (2010), 013103.
25. J. F. Li, B. Yu, L. Wang, F. C. Li, L. Hou, A mixed subgrid-scale model based on ICSM and TADM for LES of surfactant-induced drag-reduction in turbulent channel flow, App. Therm. Eng. 115 (2017) 1322-1329.
26. J. F. Li, B. Yu, Y. Zhao, Y. Wang, W. Li, Flux conservation principle on construction of residual restriction operators for multigrid method, Int. Commun. Heat Mass Transfer 54 (2014) 60–66.
27. L. Wang, Large-eddy simulation of turbulent drag-reducing flows of viscoelastic fluids, PhD thesis, Harbin: Harbin Institute of Technology, 2016.

Jingfa Li received the Doctor of Eng. degree in Petroleum Storage and Transportation Engineering from China University of Petroleum (Beijing) in 2017. He currently works as a postdoctoral fellow at Computational Transport Phenomena Laboratory (CTPL), King Abdullah University of Science and Technology (KAUST), Saudi Arabia. His research interests focus on efficient and robust algorithm for multiphase flow and turbulent flow, and model reduction method for porous media flow.

Bo Yu obtained the Doctor of Eng. degree in Engineering Thermophysics from Xi'an Jiaotong University in 1999, China. He then worked at Kyushu University from 1999 to 2001 as a postdoctoral fellow and at the National Institute of Advanced Industrial Science and Technology, Japan, from 2001 to 2005 as a special research associate. From April 2005 to October 2015, he joined China University of Petroleum (Beijing) as a full professor. Since November 2015 he severed as a full professor at Beijing Institute of Petrochemical Technology, China. His major research interests are computational heat transfer, turbulent drag-reducing flow, heat transfer enhancement and transportation technology of crude oil, etc.

Shuyu Sun received the Doctor of Eng. degree in Chemical Engineering from Tianjin University in 1997, China, and the Doctor of Philosophy degree in Computational and Applied Mathematics from the University of Texas at Austin in 2003, USA. From 2003 to 2005, he served as the postdoctoral fellow in the University of Texas at Austin. Then he joined the Department of Mathematical Sciences at Clemson University as an assistant professor in USA. Since 2009, He joined the King Abdullah University of Science and Technology (KAUST), Saudi Arabia. He is currently a co-director of the Center for Subsurface Imaging and Fluid Modeling Consortium (CSIM) and the Head of the Computational Transport Phenomena Laboratory (CTPL) at KAUST. His research interests include finite element methods and numerical analysis, computational transport phenomena, numerical oil reservoir simulations, and computational thermodynamics of reservoir fluids.

Dongliang Sun received his Doctor of Eng. degree in Engineering Thermophysics from Xi'an Jiaotong University in 2009, China. From 2009 to 2014, he served as the lecturer and associate professor in North China Electric Power University. He joined Beijing Institute of Petrochemical Technology as a full professor since 2014. His research interests focus on numerical heat transfer, multiphase flow, and energy storage technique.

Yasuo Kawaguchi received the B.Sc. degree in Mechanical Engineering in 1974, and finished the Mechanical Engineering Doctoral course Completed program in 1983 from Kyoto University, Japan. He currently is a full professor at Department of Mechanical Engineering, Tokyo University of Science, Japan. His research interests focus on Fluid engineering (Turbulence, Rheology, Multiphase flow, Heat transfer, Energy conversion).

Jingfa Li

Bo Yu

Shuyu Sun

Dongliang Sun

Yasuo Kawaguchi